Tree Physiology 30, 1001–1015
doi:10.1093/treephys/tpq054

Variable conductivity and embolism in roots and branches of four contrasting tree species and their impacts on whole-plant hydraulic performance under future atmospheric CO_2 concentration

JEAN-CHRISTOPHE DOMEC,[1,2,3] KARINA SCHÄFER,[2,4] RAM OREN,[1] HYUN S. KIM[1] and HEATHER R. McCARTHY[5]

[1] *Nicholas School of the Environment and Earth Sciences, Box 90328, Duke University, Durham, NC 27708, USA*

[2] *Corresponding authors (jc.domec@duke.edu; karinavr@andromeda.rutgers.edu)*

[3] *Department of Forestry and Environmental Resources, North Carolina State University, Raleigh, NC 27695, USA*

[4] *Federated Department of Biological Sciences, Rutgers University, Newark, NJ 07102, USA*

[5] *Department of Earth System Science, University of California, Irvine, CA 92697, USA*

Received January 12, 2010; accepted May 13, 2010; published online June 21, 2010

Summary Anatomical and physiological acclimation to water stress of the tree hydraulic system involves trade-offs between maintenance of stomatal conductance and loss of hydraulic conductivity, with short-term impacts on photosynthesis and long-term consequences to survival and growth. Here, we study the role of variations in root and branch maximum hydraulic specific conductivity ($k_{s\text{-max}}$) under high and low soil moisture in determining whole-tree hydraulic conductance (K_{tree}) and in mediating stomatal control of gas exchange in four contrasting tree species growing under ambient and elevated CO_2 (CO_2^a and CO_2^e). We hypothesized that K_{tree} would adjust to CO_2^e through an increase in root and branch $k_{s\text{-max}}$ in response to anatomical adjustments. However, physiological changes observed under CO_2^e were not clearly related to structural change in the xylem of any of the species. The only large effect of CO_2^e occurred in branches of *Liquidambar styraciflua* L. and *Cornus florida* L. where an increase in $k_{s\text{-max}}$ and a decrease in xylem resistance to embolism ($-P_{50}$) were measured. Across species, embolism in roots explained the loss of K_{tree} and therefore indirectly constituted a hydraulic signal involved in stomatal regulation and in the reduction of $G_{s\text{-ref}}$, the sap-flux-scaled mean canopy stomatal conductance at a reference vapour pressure deficit of 1 kPa. Across roots and branches, the increase in $k_{s\text{-max}}$ was associated with a decrease in $-P_{50}$, a consequence of structural acclimation such as larger conduits, lower pit resistance and lower wood density. Across species, treatment-induced changes in K_{tree} translated to similar variation in $G_{s\text{-ref}}$. However, the relationship between $G_{s\text{-ref}}$ and K_{tree} under CO_2^a was steeper than under CO_2^e, indicating that CO_2^e trees have lower $G_{s\text{-ref}}$ at a given K_{tree} than CO_2^a trees. Under high soil moisture, CO_2^e greatly reduced $G_{s\text{-ref}}$. Under low soil moisture, CO_2^e reduced $G_{s\text{-ref}}$ of only *L. styraciflua* and *Ulmus alata*. In some species, higher xylem dysfunction under CO_2^e might impact tree performance in a future climate when increased evaporative demand could cause a greater loss of hydraulic function. The results contributed to our knowledge of the physiological and anatomical mechanisms underpinning the responses of tree species to drought and more generally to global change.

Keywords: Cornus florida, embolism, FACE, Liquidambar styraciflua, Pinus taeda L., reference stomatal conductances, Ulmus alata, whole-tree hydraulic conductance.

Introduction

Although some species close stomata under elevated atmospheric CO_2 concentration (CO_2^e), photosynthesis is likely to be higher (Medlyn et al. 2001), increasing the availability of carbohydrates for growth. In forests that are well coupled to the atmosphere and experience some water limitation, stomatal closure may allow for a greater canopy leaf area (Woodward 1993). Regardless of whether CO_2^e-induced leaf area increase is due to the saving of water or simply due to increased ability to keep shaded foliage in a positive carbon balance, higher leaf area is likely to be accompanied by higher cross-sectional area of the xylem (Tyree and Alexander 1993, McCarthy et al. 2007, 2009) and higher amount of fine roots (Norby and Jackson 2000, King et al. 2001), thus not changing the relationships among the areas of the absorbing, transporting and transpiring surfaces (Pataki et al. 1998*a*). However, the extra carbohydrates invested in wood production may cause changes in wood anatomy (different conduit size) with potential effects on xylem permeability and therefore the capacity for water flux. A distinction should be made

© The Author 2010. Published by Oxford University Press. All rights reserved.
For Permissions, please email: journals.permissions@oxfordjournals.org

Downloaded from http://treephys.oxfordjournals.org at DigiTop USDA's Digital Desktop Library on August 24, 2010

between the actual xylem area defined as the total amount of sapwood present versus the functional or hydraulically active sapwood. Generally, the later is significantly lower than the former mainly because of reduced water transport capacity following cavitation-induced embolism (Tyree and Zimmermann 2002).

The effects of CO_2^e on wood properties has been scarcely investigated, and the physiological literature has insufficient information to support prediction of how CO_2^e would change plant hydraulics and affect gas exchange and plant performance. Anatomical responses to CO_2^e vary among species with a tendency toward an increase in wood density and conduit size in ring-porous species and with limited or no effect in diffuse-porous species (Conroy et al. 1988, Atkinson and Taylor 1996, Ceulemans et al. 2002, Gartner et al. 2003, Kaakinen et al. 2004, Watanabe et al. 2008). In conifers, the results are mixed, some showing that increased radial growth under CO_2^e was not accompanied by a change in wood density or cell wall thickness (Telewski et al. 1999, McCarthy et al. 2006), while others showing an increase in wood density and tracheid size (Tyree and Alexander 1993, Saxe et al. 1998). Effects of CO_2^e on wood structure and potential xylem permeability, quantified as the maximum specific conductivity of the xylem ($k_{s\text{-max}}$), would directly translate to whole-plant efficiency to transport water (Sterck et al. 2008), quantified as whole-tree hydraulic conductance (K_{tree}). Because so little is known about how $k_{s\text{-max}}$ and K_{tree} respond to CO_2^e (Saxe et al. 1998), general trends in the effects of CO_2^e on water transport capacity at the xylem or tree scale are difficult to predict.

Canopy stomatal conductance (G_s) is very sensitive and dynamically limited by K_{tree} (Comstock 2002, Meinzer 2002). Stomata control plant water status and regulate the amount of water extracted by the plant from the soil by controlling the rate of water loss to the atmosphere such that the capacity of the soil–plant hydraulic system to supply water to leaves is matched (Oren et al. 1999, Sperry 2000, Domec et al. 2009*a*). Should stomata fail to sense and respond to a lower capacity of the soil–plant system to supply water, xylem would embolize rapidly, increasing the risk of hydraulic dysfunction and dehydration of leaves (Maseda and Fernández 2006). Xylem dysfunction as a result of cavitation-induced embolism is the main factor determining the large decreases in $k_{s\text{-max}}$ recorded in stems (Tyree and Ewers 1991, Domec and Gartner 2002), roots (Sperry and Ikeda 1997, Domec et al. 2004) and, thus, in the whole plants as K_{tree} is reduced (Meinzer 2002, Domec et al. 2009*a*). However, the hydraulic conductance of each part of the water pathway (root to leaf) plays a different role in limiting water transport. Within trees, most of the hydraulic resistance resides in the root system, and roots are more vulnerable to cavitation than the trunk or branches (Sperry and Ikeda 1997, Choat et al. 2005, Domec et al. 2009*c*). This implies that compared with branches, roots are likely to represent a critical hydraulic bottleneck in whole-plant water transport.

The magnitude of plant structural and physiological responses to CO_2^e may depend on water availability (Monje and Bugbee 1998, Domec et al. 2009*c*). Under CO_2^e, changes in hydraulic characteristics may negatively impact the ability of plants to negotiate periods of water stress if the increase in xylem production is associated with larger conduits because of their lower resistant to cavitation (Hacke et al. 2006, Sperry et al. 2006). In contrast, the changes may have a positive effect on drought resistance if the increased carbon investment in xylem produces denser wood with thicker-cell-walled conduits that are more resistant to cavitation (Hacke et al. 2001*a*, Domec et al. 2009*b*). At present, the interaction effects between CO_2 and water availability on plant hydraulics, likely to differ among coexisting species of differing anatomy and physiology, are poorly understood.

The aim of this study was to quantify the effect of CO_2^e on anatomical and functional traits related to water transport, gas exchange and water economy and drought tolerance. We investigated the conditions under which embolism in the xylem of roots and branches was most likely to occur, as well as the relationships between embolism, K_{tree} and G_s. We performed this study on four species, *Pinus taeda* L. and *Liquidambar styraciflua* L. occupying the main canopy, and *Ulmus alata* and *Cornus florida* L. in the sub-canopy of the experimental plots at the Duke Forest free-air CO_2 enrichment (FACE) facility. In addition to occupying different canopy strata, the species represented different xylem types: one non-porous gymnosperm (*P. taeda*), two diffuse-porous angiosperms (*L. styraciflua* and *C. florida*) and one ring-porous angiosperm (*U. alata*). We hypothesized that different xylem anatomies should lead to a wide range of $k_{s\text{-max}}$ and K_{tree} and large difference in resistance to cavitation, allowing quantification of the link between liquid- and gas-phase transport and how it is affected by CO_2^e.

Methods

Experimental setting

The experiment is located in a loblolly pine (*P. taeda*) plantation established in 1983 on low fertility, acidic clay-loam of the Enon series, in the Blackwood Division of Duke Forest, North Carolina (35°58′ N, 79°08′ W). The experimental site was clear-cut in 1982, to remove a 50-year-old mixed pine forest, and replanted in 1983. The 32-ha experimental forest of loblolly pine is derived from 3-year-old, half-sibling seedlings planted in 2.4 × 2.4 m spacing. The study focused on three plots exposed to ambient CO_2 and three plots targeted at + 200 μmol mol^{-1} CO_2 above ambient. Each elevated CO_2 plot was paired with an ambient plot, thus yielding $n = 3$ paired treatment blocks (Schäfer et al. 2002, Schäfer 2009). CO_2 enrichment is implemented according to the FACE protocol (Hendrey et al. 1999). In 1996, when CO_2 enrichment started, the pine trees had grown to ~12 m height, reaching 15 m in 2000 (Table 1), and accounted for 89% of the basal area (McCarthy et al. 2007). The prevailing codominant species is *L. styraciflua*, and the most common sub-

Downloaded from http://treephys.oxfordjournals.org at DigiTop USDA's Digital Desktop Library on August 24, 2010

Table 1. Range of diameter at 1.35 m (DBH) of individuals measured, range in height (h) and individual projected leaf-to-sapwood area ratio (A_L:A_S) under ambient (CO_2^a) or elevated (CO_2^e) CO_2 concentration at the Duke FACE site, NC.

Species	Year	Treatment	DBH (mm)	h (m)	A_L:A_S (m^2 cm^{-2})
Pinus taeda	2007	CO_2^a	187–223	17.4–19.6	0.15–0.16
	2007	CO_2^e	210–243	17.2–18.4	0.17–0.22
Pinus taeda	2000	CO_2^a	147–183	13.7–15.2	0.12–0.13
	2000	CO_2^e	169–189	14.6–15.8	0.13–0.14
Ulmus alata	2000	CO_2^a	48–88	5.4–7.8	0.57–0.82
	2000	CO_2^e	43–63	5.1–6.3	0.73–0.86
Liquidambar styraciflua	2000	CO_2^a	41–55	4.7–6.3	0.29–0.40
	2000	CO_2^e	40–56	4.6–6.4	0.27–0.42
Cornus florida	2000	CO_2^a	42–55	4.9–5.8	0.24–0.25
	2000	CO_2^e	34–52	4.1–5.6	0.24–0.27

canopy species are *Acer rubrum*, *U. alata* and *C. florida*. In 2000, the projected leaf area index of pine was 4.0 m^2 m^{-2} (Schäfer et al. 2002), and the stand was just beginning to enter a stage of competitive self-thinning. Mean annual temperature is 15.8 °C, and mean annual precipitation is 1145 mm, usually evenly distributed throughout the year. Summers are warm and humid, and the growing season mean temperature is 22.1 °C. Further site information can be found in Oren et al. (1998*a*; http://face.env.duke.edu).

Environmental parameters such as air temperature (T_a) and relative humidity (Vaisala HMP 35C, Helsinki, Finland) were measured in the upper third of the canopy and used to calculate the vapour pressure deficit (D). Soil water potential (Ψ_s) measurements were monitored continuously in each plot using one equitensiometer per plot (EQ2, Delta-T-Devices, Cambridge, UK). Previous work at the site showed that soil physical characteristics and root distribution are uniform throughout a given plot and that one probe can provide representative values of Ψ_s (Schäfer 2009). In addition to Ψ_s, soil moisture was measured with frequency domain reflectometry (CS615 Campbell Scientific, Logan, UT) with four randomly placed probes in each plot. The probes extended to 30–40 cm from the surface, integrating through most of the rooting zone (Oren et al. 1998*a*). All measurements were logged every 30 s, and 30-min averages were stored in a digital data logger (21X or 23X, Campbell Scientific, Logan, UT).

Sap-flux measurements and mean-crown stomatal conductance

In 2000, sap flux and transpiration were measured in all species. In 2007, they were also measured in *P. taeda* to detect any long-term effects of CO_2^e on the dominant species. We could not work with the other species in 2007 because the stand had reached full canopy closure and was in an advanced stage of competitive self-thinning with few individuals left.

Sap-flux density was measured in eight *P. taeda*, four *L. styraciflua* and five *U. alata* in each plot. For *C. florida*, only five trees of adequately large diameter for sap-flux measurements (≥30 mm in diameter) were available to represent each of the CO_2^e or the ambient CO_2 (CO_2^a) treatments. The size range (height and diameter) of the trees used for sap measurements is shown in Table 1. Sap flow was measured at breast height with 20-mm Granier-type heat dissipation sensors (Granier 1987). Sensor operation at the FACE site is detailed in Schäfer et al. (2002). The sensor signal was converted to sap-flux density (J_s in g m^{-2} s^{-1}) according to Granier (1987), adjusting the baseline for the effect of night transpiration (Oishi et al. 2008) and scaled to a tree-scale average transpiration per unit leaf area (E, in mmol m^{-2} s^{-1}; Oren et al. 1998*b*, Schäfer et al. 2002). In larger *P. taeda* trees, sensors were also placed deeper in the sapwood to account for radial patterns and scaled accordingly (see Schäfer et al. 2002). The sap-flux-based G_s (mmol m^{-2}_{leaf} s^{-1}) was calculated from E and D, using the simplified inversion of the Penman–Monteith model (Monteith and Unsworth 1990, Köstner et al. 1992). This approach was valid because in all treatments D was close to the leaf-to-air vapour pressure deficit due to high boundary-layer conductance indicating that the forest is well coupled to the atmosphere such that stomata control transpiration (Schäfer et al. 2003). Indeed, given that >90% of the daytime canopy wind speed was >0.7 m s^{-1}, and that leaf dimensions do not exceed 0.06 m, we calculated using the equation described in Jones (1992) that the mean daytime boundary-layer conductance averaged 65 times G_s of the *P. taeda* and between 15 and 9.6 of the deciduous species. This finding is consistent with previous studies in this stand and adjacent broadleaf deciduous forest (Phillips et al. 1997, Pataki and Oren 2003, Oishi et al. 2008). Mean values of G_s were calculated only under conditions of $D \geq 0.6$ kPa to avoid the large relative errors associated with sap-flux-scaled conductance calculated at D below this threshold (Ewers and Oren 2000).

Sapwood area and leaf area are required for calculating E and thus mean G_s (Table 1). For each species, sapwood area was estimated from allometric equations relating outside bark diameter to sapwood area (Kim 2009, Schäfer 2009). The trees equipped with sap flow sensors were within the size range of the trees that were used to develop the equations. For the deciduous species, we used relationships between

Downloaded from http://treephys.oxfordjournals.org at DigiTop USDA's Digital Desktop Library on August 24, 2010

diameter and leaf area derived from harvested trees to estimate leaf area. We used trees growing under ambient conditions to estimate leaf area under both CO_2 environments because it has been shown that allometric relationships between stem diameter and leaf area are not affected by CO_2^e (Pataki et al. 1998*b*, Schäfer et al. 2002, McCarthy et al. 2007). *P. taeda* carries 2 years of foliage during the growing season, with a higher proportion of previous-year needles in spring when soil moisture is high and a higher proportion of current-year needles in late summer when soil moisture is low. Therefore, for this species, we used the leaf area data from McCarthy et al. (2007) for 2000 and from Novick et al. (2009) for 2007, separating the contribution of both needle cohorts and thus accounting for the seasonal leaf area dynamics under CO_2^a and CO_2^e conditions. Leaf area values used were projected or one-sided leaf area.

Analysis of the response of stomatal conductance to changes in driving force

Stomata of isohydric plants respond to D in a manner consistent with protecting xylem integrity and thus capacity for water transport. The emerging behaviour is decreasing G_s with increasing D at a rate that is predictable and proportional to G_s at low D (Oren et al. 1999). Thus, G_s data from each treatment were analysed based on:

$$G_s = b - m \times \ln(D) \quad (1)$$

where b is G_s at D = 1 kPa (hereafter designated as reference stomatal conductance, $G_{s\text{-ref}}$), and m is the sensitivity of G_s to D ($-dG_s/d\ln D$, in mmol m^{-2} s^{-1} $(\ln kPa)^{-1}$). Based on the stated hydraulic consideration, $-dG_s/d\ln D$ is proportional to $G_{s\text{-ref}}$ with the proportionality averaging ~0.60 and varying predictably depending on the range of D used in the analysis (Oren et al. 1999, Kim et al. 2008, Ward et al. 2008, Domec et al. 2009*c*). In stands with high daytime boundary-layer conductance, it has been shown that the relationship between reference stomatal conductance and the stomatal sensitivity to D of leaf-based stomatal conductance (g_s) is similar to that of sap-flow derived G_s (Addington et al. 2004, Kim et al. 2008, Domec et al. 2009*a*).

Hydraulic properties of shoots and roots and whole-tree hydraulic conductance

Aiming to ensure long-term integrity of the Duke FACE experiment, destructive harvest was not allowed within the six experimental plots: thus, plant material was collected in the previously established prototype ring, which has been enriched with CO_2 during daytime of the growing season since 1993 (Ellsworth et al. 1995, Oren et al. 2001). Plant material grown under CO_2^a was collected from the surrounding area. For each species, six roots (1.6–4.1 mm diameter) dug from the upper soil layer (10–25 cm) and eight branches (2.8–7.6 mm diameter) accessed from the upper third of the canopy were collected within a 2-week period in July to avoid seasonal differences in vulnerability curves caused by cavitation fatigue (Hacke et al. 2001*b*). The segments were used first to calculate maximum specific conductivity ($k_{s\text{-max}}$), which was calculated as the mass flow rate of the perfusion solution divided by the pressure gradient across the segment, normalized by the xylem cross-sectional area. Removal of residual air emboli was achieved by flushing the samples for 20 min with filtered water at a pressure of 150 kPa. The same segments were then used to estimate xylem vulnerability curves, which describe the relationship between the percentage of loss of $k_{s\text{-max}}$ caused by embolism through air seeding and xylem pressure (Ψ_x), obtained based on the centrifugal force technique (Alder et al. 1997). The centrifuge (Sorvall RC5C, Thermo Fisher Scientific, Waltham, MA) had a custom-designed rotor holding 14.2-cm-long samples. From each vulnerability curve, the pressure causing a 50% (P_{50}) loss of $k_{s\text{-max}}$ was calculated by fitting a sigmoidal function to the measured points (Pammenter and Vander Willigen 1998, Domec and Gartner 2001):

$$\mathrm{PLC} = 100/(1 + e^{a(\Psi x - b)}) \quad (2)$$

where PLC is the percentage loss of $k_{s\text{-max}}$, the parameter a is an indicator of the slope of the linear part of the vulnerability curve, and the parameter b represents P_{50} (in MPa), which is widely used as an index of xylem vulnerability to embolism between (Hacke et al. 2001*a*) or within (Domec and Gartner 2002, Choat et al. 2005) species. The actual slope ($s = a25$ in PLC MPa^{-1}) of the linear part of the vulnerability curve was determined from the fitted curves (Domec and Gartner 2001). Hacke et al. (2006) showed that for vessel-bearing species with long conduits (ring-porous species), the centrifuge method is appropriate to determine vulnerability curves and compares well with the air-injection method if a low pressure head is used to measure conductivity. Therefore, in *U. alata*, we kept the magnitude of the pressure head below 100 kPa m^{-1} (pressure head of 7.5 kPa) because higher gradients would have reversed embolism during the course of a measurement by flushing gas bubbles out of the vessels that were continuous through the segments.

Percentage loss of $k_{s\text{-max}}$ in the field was estimated for roots and branches by relating the vulnerability curves to either Ψ_s or midday leaf water potentials (Ψ_l), respectively. We used field values of water potential measured in 2000 under high soil moisture (between March and April when $\theta > 0.3$ $m^3 m^{-3}$) and under low soil moisture (between mid-August and late September when $\theta < 0.18$ $m^3 m^{-3}$). During the 2000 growing season for each species and during the 2007 growing season for *P. taeda*, values of Ψ_l were obtained from three to five fully expanded leaves per treatment plot every 2–3 weeks, thus capturing a range of seasonally varying environmental conditions. Leaves were sampled from the upper third of the canopy. The cut leaf was placed in a plastic bag in the shade to avoid further evaporation; Ψ_l measurements were conducted within 5 min of harvest using a pressure chamber (PMS instruments, Corvallis, OR).

Downloaded from http://treephys.oxfordjournals.org at DigiTop USDA's Digital Desktop Library on August 24, 2010

To analyse the effect of $k_{s\text{-max}}$ as well as shoot and root hydraulic conductivity on whole-tree hydraulic conductance (K_{tree}), K_{tree} was calculated as:

$$K_{tree} = E/(\Psi_s - \Psi_l) \quad (3)$$

where late morning (1000–1130 h) values of Ψ_l and E (see Table 1 for size and height of trees) were used because at this time light is saturating and leaves are likely to have transpired all stored water so that steady-state water flow conditions in the stem are likely to exist (Loustau et al. 1998).

Light microscopy observations of tracheid dimensions

We made transverse sections from each of the wood samples that had been used to measure $k_{s\text{-max}}$ and to produce vulnerability curves. Those sections were stained with safranin-O and mounted in glycerin for image analysis using Image-Pro (Media Cybernetics, Silver Spring, MD). To account for the disproportionate contribution of large conduits to total flow, the first step was to estimate tracheid diameter distributions for calculation of mean hydraulic diameter ($=\Sigma d^5/\Sigma d^4$, where d = individual conduit diameter, Kolb and Sperry 1999). Conduit lumen diameters were calculated by measuring conduit sizes on pith–cambium transects. For each sample separately, six radial files of conduits were randomly selected, and the diameter of all tracheids or vessels was measured. Total conductivity of a cross-section is determined by the aggregate conductivity through a population of conduits, some transporting water and others not. The tension required to cause 50% loss of $k_{s\text{-max}}$, P_{50}, is the point at which the conduits, with diameters that represent the mean hydraulic diameter, embolize (Kolb and Sperry 1999), and no transport occurs through these or larger diameter conduits.

Hacke et al. (2001*a*) calculated that embolized conduits experience large bending stresses that could lead to cell collapse under drought conditions. The basis for this relationship is that the double cell wall shared by adjacent cells behaves in a manner similar to a long plate of width b (cell diameter) and thickness t (double-cell-wall thickness), and this plate will buckle under a force proportional to $(t/b)^2$ (Hacke et al. 2001*a*). Therefore, after determining mean hydraulic diameter for a section, we estimated $(t/b)^2$ for each sample on tracheids or vessels with diameters within 10% of the mean hydraulic diameter. About 90–120 conduits per sample were used to measure t and b. Furthermore, Hacke et al. (2001*a*) showed that $(t/b)^2$ calculated from cell anatomical dimensions are correlated with the overall sample wood density. To test whether any changes in wood density associated with species, organ or treatment were linked to changes in $(t/b)^2$, P_{50} or $k_{s\text{-max}}$ (Hacke et al. 2001*a*), we measured wood density (g cm^{-3}) of each sample tested hydraulically. Wood density was calculated as the ratio of dried weight over fresh volume. Wood samples were oven-dried at 65 °C for 48 h, and fresh volume was determined by Archimedes' principle.

Hydraulic conductance of wood is a function of both the tracheid lumen conductance and bordered pit conductance. We estimated the specific conductivity of the pits, which represents the parallel conductivity of pits ($k_{s\text{-pit}}$) on a tissue basis (rather than for individual pits) to be able to link it to P_{50} and to pit hydraulic efficiency. Measured $k_{s\text{-max}}$ was assumed to represent the joint conductivity of both lumen and pits ($k_{s\text{-lumen}}$ and $k_{s\text{-pit}}$, respectively), and thus $k_{s\text{-pit}}$ could be calculated as:

$$k_{s\text{-pit}} = (1/k_{s\text{-max}} - 1/k_{s\text{-lumen}})^{-1} \quad (4)$$

where $k_{s\text{-lumen}}$ was calculated according to the Hagen–Poiseuille equation for capillaries using conduit diameter and conduit density (Ewers 1985).

Statistical analysis

The effects of CO_2^e on K_{tree} and $G_{s\text{-ref}}$ were tested based on an analysis of variance (ANOVA) where individual plots were used as replicates. Due to low and uneven distribution of the monitored *C. florida* individuals and recognizing that between-tree variance is often larger than among-plot variance (Oren et al. 1998*b*), analyses of data for this species were made at the individual tree level rather than at the plot level. Means of anatomical and physiological data measured on excised samples were compared among treatments with *t*-tests. Probability levels $P < 0.05$ and $P < 0.10$ were considered to indicate either a very clearly or a clearly discernible CO_2^e effect, respectively. Statistical analyses were performed using SAS (version 9.1, Cary, NC), and curve fits were performed using SigmaPlot (version 9.0, SPSS Inc. San Rafael, CA).

Results

Values of $k_{s\text{-max}}$ (conductivity with embolism removed) for a given species decreased from roots to branches ($P = 0.01$). Branches of all three angiosperm species had higher $k_{s\text{-max}}$ than the conifer species ($P = 0.03$). Although branch samples in CO_2^e had smaller conduit diameter in *U. alata* and larger conduit diameter in *C. florida* (Table 2), there was only a CO_2^e effect on $k_{s\text{-max}}$ in *C. florida.* Roots of *C. florida* and *P. taeda* had larger conduit diameters in CO_2^e than in CO_2^a. This trend was only reflected in an effect on $k_{s\text{-max}}$ in *P. taeda* (Table 2).

Roots were more vulnerable to cavitation (less negative P_{50}) than branches in all species (Table 2, Figure 1), and in all species but *P. taeda*, root xylem vulnerability curves were steeper than branch vulnerability curves ($P < 0.04$) (Table 2), with PLC increasing sharply above 0.25 MPa (Figure 1). Branches of *C. florida* and *L. styraciflua* grown under CO_2^e had higher vulnerability to cavitation than those growing under CO_2^a (Figure 1B and D). Branches of the three angiosperms showed an overall higher vulnerability to cavitation under CO_2^e (multivariate analysis of variance (MANOVA), $P = 0.004$). Roots of the three angiosperms showed an overall

Downloaded from http://treephys.oxfordjournals.org at DigiTop USDA's Digital Desktop Library on August 24, 2010

Table 2. Hydraulic characteristics of roots and branches of the four woody species growing under ambient or elevated CO_2 concentration at the Duke FACE site, NC: maximum hydraulic specific conductivity, air-seeding pressure (resistance to embolism, P_{50}), slope of the linear part of the vulnerability curve centred on P_{50} (s), conduit diameter, contribution of end-wall resistivity to total conduit resistivity and conduit thickness-to-span ratio (t/b). Probability levels in bold were considered to indicate a very clearly ($P < 0.05$) or a clearly ($P < 0.10$) discernible CO_2^e effect. Lumen hydraulic conductivity can be calculated as: $k_{s\text{-lumen}} = k_{s\text{-max}}/(1 - k_{s\text{-max}}/_{s\text{-pit}})$.

	Branches			Roots		
	CO_2^a	CO_2^e	P	CO_2^a	CO_2^e	P
Maximum hydraulic specific conductivity ($ks_{\text{-max}}$, kg m^{-1} s^{-1} MPa^{-1})						
Pinus taeda	0.34 ± 0.02	0.47 ± 0.03	0.13	0.75 ± 0.06	1.76 ± 0.21	**0.06**
Ulmus alata	2.73 ± 0.18	2.53 ± 0.27	0.92	4.66 ± 0.15	6.16 ± 1.34	**0.09**
Liquidambar styraciflua	1.33 ± 0.15	1.71 ± 0.23	**0.04**	2.43 ± 0.25	1.54 ± 0.22	0.29
Cornus florida	1.15 ± 0.12	1.93 ± 0.17	**0.02**	0.20 ± 0.01	0.24 ± 0.02	0.45
Air-seeding pressure (P_{50}, MPa)						
Pinus taeda	−3.3 ± 0.1	−3.4 ± 0.3	0.37	−0.61 ± 0.11	−1.11 ± 0.22	**0.04**
Ulmus alata	−0.4 ± 0.1	−0.4 ± 0.2	0.95	−0.13 ± 0.12	−0.27 ± 0.16	0.42
Liquidambar styraciflua	−2.0 ± 0.2	−1.1 ± 0.2	**0.09**	−0.12 ± 0.01	−0.29 ± 0.09	**0.04**
Cornus florida	−3.9 ± 0.4	−2.9 ± 0.4	**0.04**	−1.02 ± 0.37	−1.16 ± 0.46	0.69
Slope (s, PLC MPa^{-1})						
Pinus taeda	66 ± 9	53 ± 6	0.19	68 ± 3	47 ± 2	**0.03**
Ulmus alata	56 ± 14	59 ± 13	0.34	213 ± 24	192 ± 22	**0.10**
Liquidambar styraciflua	30 ± 2	52 ± 4	**0.02**	250 ± 31	101 ± 23	**0.02**
Cornus florida	18 ± 2	19 ± 3	0.26	40 ± 6	36 ± 13	0.16
Conduit diameter (μm)						
Pinus taeda	19 ± 1	22 ± 1	0.16	25 ± 1	33 ± 3	**0.03**
Ulmus alata	35 ± 1	29 ± 2	**<0.01**	45 ± 4	47 ± 5	0.72
Liquidambar styraciflua	30 ± 2	33 ± 2	0.87	60 ± 3	54 ± 4	0.17
Cornus florida	31 ± 2	34 ± 1	**0.09**	30 ± 2	37 ± 1	**0.03**
Contribution of end-wall resistivity to total conduit resistivity ($k_{s\text{-max}}/k_{s\text{-pit}}$, %)						
Pinus taeda	62 ± 5	50 ± 6	**0.04**	71 ± 3	77 ± 4	**0.07**
Ulmus alata	62 ± 8	64 ± 5	0.76	63 ± 4	67 ± 5	0.56
Liquidambar styraciflua	41 ± 5	40 ± 3	0.81	73 ± 2	81 ± 9	0.08
Cornus florida	45 ± 4	42 ± 7	0.96	71 ± 7	72 ± 8	0.98
Conduit thickness-to-span ratio (t/b) 2×10^{-3}						
Pinus taeda	53 ± 5	54 ± 5	0.69	16 ± 1	23 ± 3	**0.02**
Ulmus alata	13 ± 1	12 ± 1	0.92	18 ± 1	19 ± 2	0.21
Liquidambar styraciflua	12 ± 1	11 ± 1	0.89	10 ± 2	14 ± 1	**0.06**
Cornus florida	12 ± 1	11 ± 1	0.81	16 ± 1	13 ± 2	0.13

shallower slope of vulnerability curve under CO_2^e (MANOVA, $P = 0.02$). CO_2^e affected root xylem vulnerability to cavitation only in *P. taeda* and *L. styraciflua*. The conduit thickness-to-span ratio $(t/b)^2$ was higher only in *P. taeda* roots, although a trend was apparent also in *L. styraciflua*, and for both species this corresponded to a more negative P_{50}. There was a positive relationship ($P = 0.01$) between wood density and $(t/b)^2$ among roots and branches of the diffuse-porous species (data not shown).

Across species, higher lumen resistivity ($1/k_{s\text{-lumen}}$) was associated with higher end-wall resistivity ($1/k_{s\text{-pit}}$). However, the increase in $1/k_{s\text{-lumen}}$ for a given increase in $1/k_{s\text{-pit}}$ was higher in branches than in roots (Figure 2A). In *C. florida* and *P. taeda*, $1/k_{s\text{-lumen}}$ and $1/k_{s\text{-pit}}$ were lower under CO_2^e ($P < 0.035$). Among roots and branches pooled together, $k_{s\text{-max}}$ was more limited by the end-wall resistance than by conduit lumen resistance, as reflected in $1/k_{s\text{-pit}}$ representing 66% of $1/k_{s\text{-max}}$. P_{50} increased more with $k_{s\text{-max}}$ in branches than in roots (Figure 2B). Among species in both treatments, there was also a negative relationship between conduit diameter and P_{50} (Figure 3A) and a positive relationship between wood density and P_{50} (Figure 3B).

The rate of decrease in k_s with the xylem pressure ($dk_s/d\Psi$) differed among species and treatments and increased with $k_{s\text{-max}}$ (Figure 4). This result indicates greater sensitivity of k_s to xylem pressure as $k_{s\text{-max}}$ increases. Among species, $dk_s/d\Psi$ was steeper in roots than in branches ($P = 0.035$).

Analysing the four species together, roots were more embolized than branches ($P = 0.01$); this was supported by intra-species analysis for all but *U. alata*, which exhibited a similar degree of native embolism in both organs over the growing season ($P = 0.23$; Figure 5). The PLC observed in branches of the four species ranged from 4% to 70% in May–June (high soil moisture), increasing to 10–80% in August–September (low soil moisture) with maximum xylem dysfunction occurring in *L. styraciflua* and *U. alata* (Figure 5). The ring-porous species (*U. alata*) experienced higher seasonal fluctuations in root embolism than the other species. In roots, PLC ranged from 25% to 85% in May–June, increasing to 55–95% in August–September (Figure 5). Averaged over both treatments,

Downloaded from http://treephys.oxfordjournals.org at DigiTop USDA's Digital Desktop Library on August 24, 2010

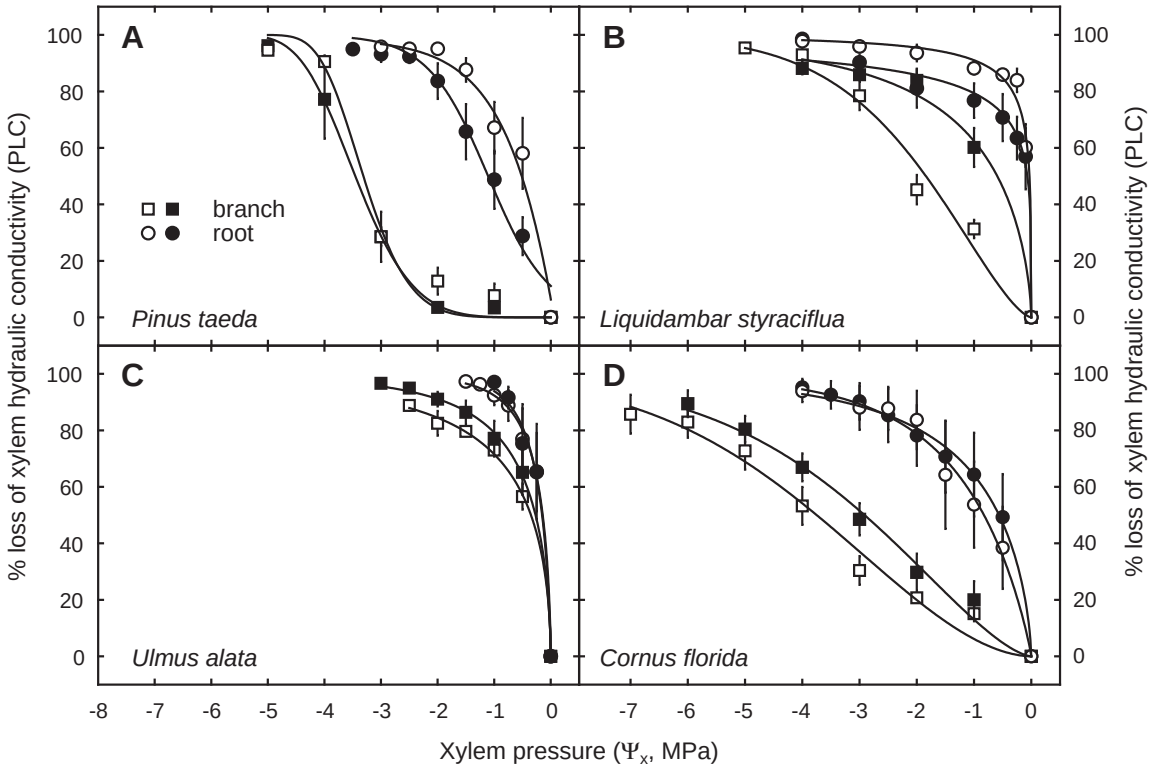

Figure 1. Vulnerability curves in (A) *P. taeda*, (B) *L. styraciflua*, (C) *U. alata* and (D) *C. florida*, showing the relationship of percentage loss of hydraulic conductivity in xylem and xylem pressure of roots and branches of trees growing under ambient (open symbols) and elevated CO_2 concentration (closed symbols). Standard errors are shown for means of n = 5–7.

PLC under low soil moisture increased by 13% in branches and 20% in roots ($P < 0.02$). Averaged over both periods, branches had 12% higher PLC under CO_2^e than under CO_2^a ($P = 0.07$). In roots of *P. taeda*, CO_2^e caused 29% ($P = 0.03$) and 22% ($P = 0.02$) lower PLC in May–June and August–September, respectively.

Reflecting substantial embolism of roots, whole-tree conductance (K_{tree}) decreased with decreasing soil moisture (Figures 5 and 6). Averaged over all species, K_{tree} of trees growing under CO_2^a declined 27% from May to September ($P = 0.07$) and even more (37%) under CO_2^e ($P = 0.04$). The largest seasonal change in K_{tree} occurred in *C. florida* and *P. taeda*, decreasing 44% and 42%, respectively (Figure 5).

Species differences were also apparent in K_{tree}, with higher values in *L. styraciflua* than in *U. alata* or *C. florida* ($P < 0.05$) (Figure 5). The $G_{s\text{-ref}}$ of all species of both treatments and both measurement periods increased proportionally with K_{tree} (Figure 7). However, the relationship between $G_{s\text{-ref}}$ and K_{tree} for trees growing under CO_2^a was steeper ($P = 0.02$) than for trees growing under CO_2^e, meaning that $G_{s\text{-ref}}$ at a given K_{tree} is lower under CO_2^e than under CO_2^a. In the angiosperm species, $G_{s\text{-ref}}$ was lower under CO_2^e than under CO_2^a when soil moisture was not limiting (Table 3, Figure 8). We only observed a marginal CO_2 × soil moisture interaction effect on $G_{s\text{-ref}}$ in *U. alata* ($P = 0.07$).

In *P. taeda*, the species for which we had data for two different years, under low soil moisture, $G_{s\text{-ref}}$ was similar in CO_2^a and CO_2^e plots in either year. However, under high soil moisture, $G_{s\text{-ref}}$ was not affected by CO_2^e in 2000, whereas in 2007 $G_{s\text{-ref}}$ was lower under CO_2^e than under CO_2^a. In 2007, the decline of $G_{s\text{-ref}}$ with soil moisture was more pronounced in the CO_2^a plots (40%) than in the CO_2^e plots (24%) (Figure 8).

Discussion

There have been few studies on the effects of CO_2^e on tree hydraulics and xylem anatomy and their downstream effect on gas exchange. This study contributes new insights to the effect of CO_2^e on $k_{s\text{-max}}$ and the relationship between treatment-induced seasonal variation in K_{tree} and gas exchange. At the cell level, constraints on relationships between conduit structure and function led to a trade-off of efficiency against safety of water transport, a trade-off that was still maintained under CO_2^e. At the plant level, the similarity of trends in liquid- and gas-phase conductances implies that functional adjustments under CO_2^e contributed to homeostasis in the operation of the hydraulic regulatory systems.

Roots as hydraulic bottlenecks: do stomata sense root xylem embolism?

The results of this study show that across four contrasting tree species, the seasonal decline in $G_{s\text{-ref}}$ was strongly related to

Downloaded from http://treephys.oxfordjournals.org at DigiTop USDA's Digital Desktop Library on August 24, 2010

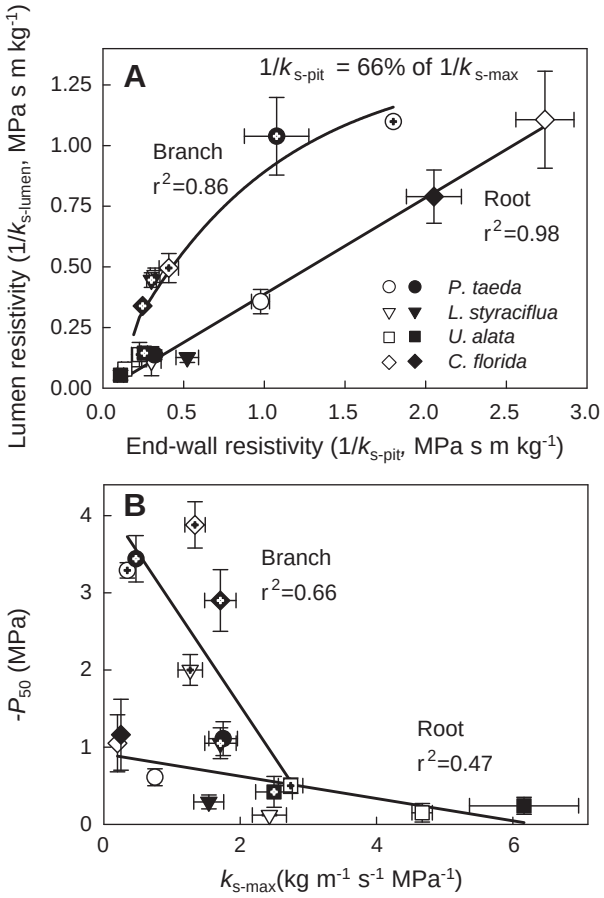

Figure 2. Relationships of (A) lumen resistivity and end-wall resistivity; (B) air-seeding pressure (pressure causing 50% loss of conductivity, P_{50}) and maximum hydraulic specific conductivity ($k_{s\text{-max}}$) in root (plain symbols) and branch (dotted symbols) samples from four co-occurring species growing under either ambient (open symbols) or elevated (closed symbols) CO_2 concentrations. All P values associated with the fitted curves are <0.02.

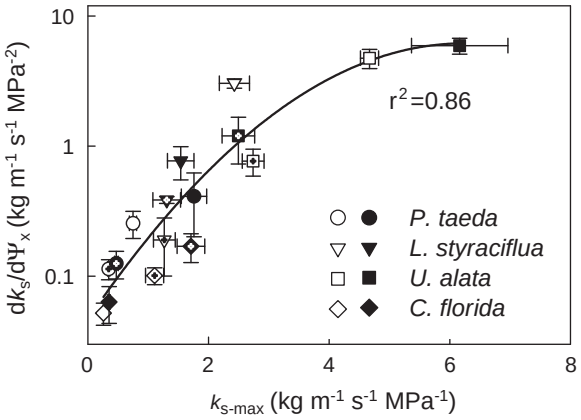

Figure 4. Relationship between the slope of the response of hydraulic conductivity (k_s) to xylem pressure (Ψ_x) and $k_{s\text{-max}}$, in root (plain symbols), and branch (dotted symbols) samples from four co-occurring species growing under either ambient (open symbols) or elevated (closed symbols) CO_2 concentrations. The P value associated with the fitted curve is <0.001.

the seasonal decline in K_{tree} indicative of a hydraulic effect on stomata regulation. This contrasts with the current view that CO_2^e directly causes stomatal closure (Ainsworth and Rogers 2007). Thus, K_{tree} acted in concert with stomata to limit water loss under conditions of low soil moisture content, which maintained Ψ_l above critical values that would have induced complete loss of hydraulic capacity (Meinzer 2002). Many studies have examined the relationships between K_{tree} and G_s (e.g., Tyree and Ewers 1991, Addington et al. 2004, Kim et al. 2008, Domec et al. 2009*a*), yet the causes of variation in K_{tree} are rarely studied. Reduced K_{tree} of trees growing under CO_2^e has seldom been investigated or detected (Kupper et al. 2006, Domec et al. 2009*c*). Here, we show that CO_2-induced differences in K_{tree} of all species were largely a reflection of the loss of root $k_{s\text{-max}}$ over a wide range of seasonal water variability (Figure 6). The dependence of K_{tree} on root hydraulic failure reflects the fact that the short portion of the pathway through the root constitutes a major portion of the whole-tree hydraulic resistance to water flow and that

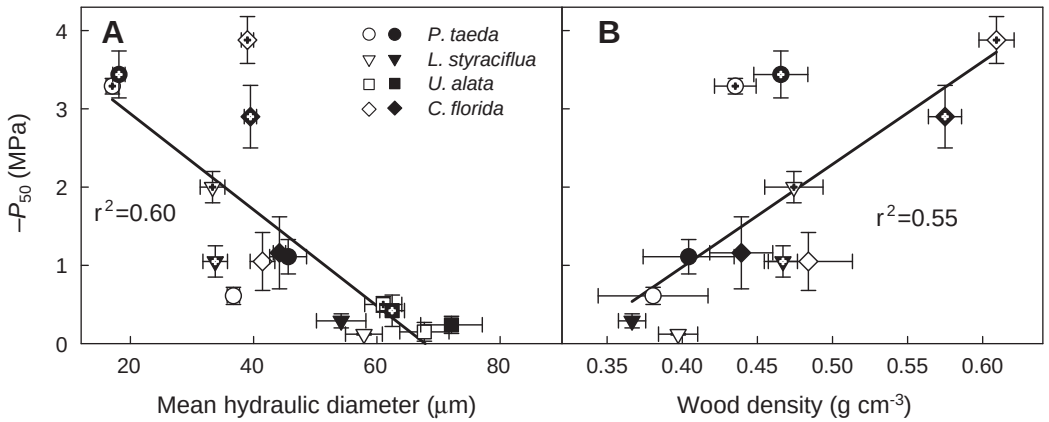

Figure 3. Relationships of (A) air-seeding pressure (pressure causing 50% loss of conductivity, P_{50}) and mean hydraulic diameter and (B) P_{50} and wood density in root (plain symbols) and branch (dotted symbols) samples from four co-occurring species growing under either ambient (open symbols) or elevated (closed symbols) CO_2 concentrations. All P values associated with the fitted curves are <0.01.

Downloaded from http://treephys.oxfordjournals.org at DigiTop USDA's Digital Desktop Library on August 24, 2010

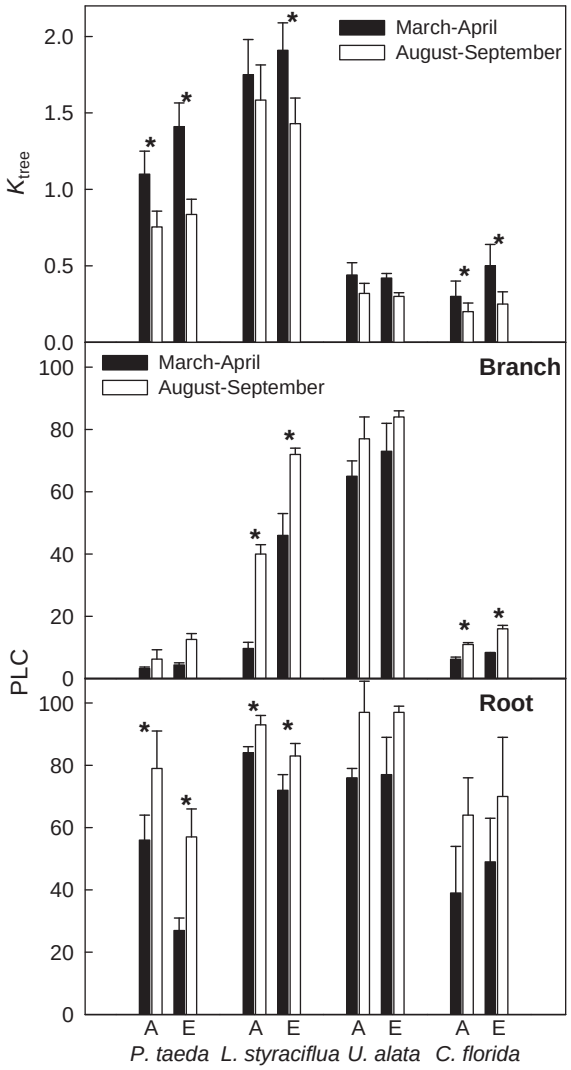

Figure 5. Whole-tree hydraulic conductance (K_{tree}) and PLC at the beginning (March–April) and at the end (August–September) of the 2000 growing season in four species growing under ambient (A) and elevated (E) CO_2. Loss of conductivity was measured using root and branch vulnerability curves to drought-induced embolism (Figure 1), and predawn and midday water potentials. Stars denote a large difference between seasonal periods ($P < 0.05$).

root hydraulic conductance greatly declines with soil moisture (Hacke et al. 2000, Comstock 2002, Domec et al. 2009*a*, 2009*c*).

As expected, the roots emerged as potentially the most vulnerable component of the xylem reflected in the higher predicted rate of hydraulic conductivity loss in field conditions (Figures 1 and 5, Sperry et al. 1998, Meinzer et al. 2009). As shown (Cochard et al. 2002), the magnitude of xylem water depletion and refilling can constitute a hydraulic signal involved in stomatal regulation. This stomatal closure would prevent Ψ_l from declining to values that could provoke embolism in stems where embolism reversal may not be as efficient as in roots (McCully 1998, Domec et al. 2004, Domec et al. 2006).

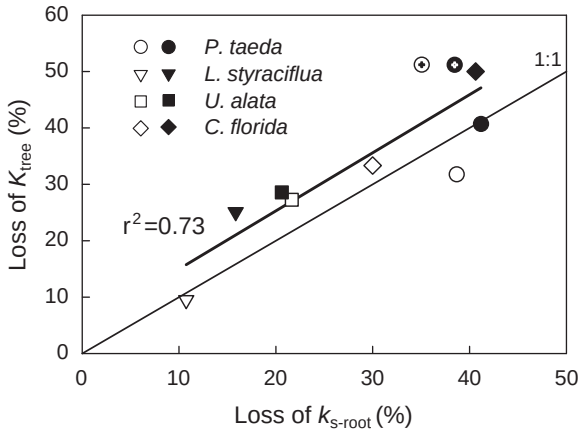

Figure 6. Effect of seasonal loss of root conductivity ($k_{s\text{-root}}$) on whole-tree hydraulic conductance (K_{tree}) in trees growing under either ambient (open symbols) or elevated (closed symbols) CO_2 concentrations ($P = 0.036$). Dotted symbols represent roots of *P. taeda* sampled in 2007. All other samples were taken in 2000.

Effects of increased CO_2 concentration on conductivity and resistance to embolism

In this study, resistance to embolism (lower P_{50}) increased at the cost of a decrease in $k_{s\text{-max}}$ (as was previously shown for *P. taeda*; Ewers et al. 2000) mainly through a reduction in $k_{s\text{-pit}}$ (Figure 2A). At the tissue level, a trade-off between water transport efficiency and resistance to water stress-induced embolism has been hypothesized (Tyree and Ewers 1991). At the species level, CO_2^e resulted in higher $k_{s\text{-max}}$ and lower resistance to embolism in either the branches or the roots but not

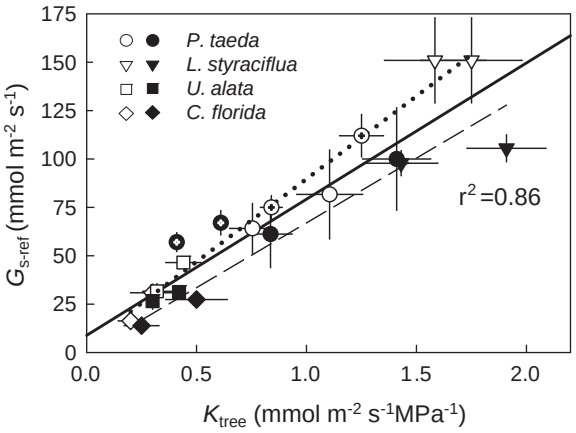

Figure 7. Effect of whole-tree hydraulic conductance (K_{tree}) on reference canopy stomatal conductance ($G_{s\text{-ref}} = G_s$ at $D = 1$ kPa, Oren et al. 1999) in trees growing under either ambient (open symbols) or elevated (closed symbols) CO_2 concentrations ($P < 0.001$). Dotted symbols represent roots of *P. taeda* sampled in 2007. All other samples were taken in 2000. Data encompass two soil moisture conditions (<18% m^3 m^{-3} and >30% m^3 m^{-3}). The relationship between $G_{s\text{-ref}}$ and K_{tree} was steeper ($P = 0.02$) for trees growing under CO_2^a (dotted line, slope = 84 ± 6) than for trees growing under CO_2^e (dashed line, slope = 55 ± 7).

Downloaded from http://treephys.oxfordjournals.org at DigiTop USDA's Digital Desktop Library on August 24, 2010

Table 3. Canopy reference stomatal conductance (Gs-ref, mmol m^{-2} s^{-1}) under high (>30% m^3 m^{-3}) and low (<18% m^3 m^{-3}) soil moisture content of the four woody species growing under ambient or elevated CO_2 concentration at the Duke FACE site, NC. Except for *P. taeda*, measured in both 2000 and 2007, all other species were sampled only in 2000. Probability levels in bold were considered to indicate a very clearly ($P < 0.05$) or a clearly ($P < 0.10$) discernible CO_2^e effect. Only *U. alata* (2000) and *P. taeda* (2007 but not 2000) showed a CO_2 × soil moisture interaction effect on $G_{s\text{-ref}}$ ($P = 0.007$ and $P = 0.003$, respectively).

	High soil moisture			Low soil moisture		
	CO_2^a	CO_2^e	P	CO_2^a	CO_2^e	P
$G_{s\text{-ref}}$, mmol m^{-2} s^{-1}						
Pinus taeda (2007)	112 ± 11	71 ± 6	**0.01**	67 ± 6	57 ± 5	0.68
Pinus taeda	83 ± 17	97 ± 12	0.23	64 ± 7	59 ± 8	0.51
Ulmus alata	46 ± 3	31 ± 3	**0.01**	32 ± 3	26 ± 4	**0.09**
Liquidambar styraciflua	151 ± 21	106 ± 7	**0.01**	151 ± 19	99 ± 6	**0.04**
Cornus florida	33 ± 1	24 ± 2	**0.001**	16 ± 1	14 ± 1	0.67

in both (Table 2). These physiological results were inconsistent with the inferences drawn from the anatomical data because trees grown in CO_2^e did not always exhibit higher conduit diameter than plants grown in CO_2^a. For embolism resistance, however, the anatomical changes were consistent with the physiological responses as reflected in the decrease of P_{50} with increasing conduit diameter (Figure 3A). Because all of the water that ascends within xylem must pass through the bordered pits of overlapping conduits, pit characteristics are a major determinant of $k_{s\text{-max}}$ (Pittermann et al. 2005), accounting for more than 50% of total xylem hydraulic resistance across a broad range of tracheid- and vessel-bearing species (Choat et al. 2008). Larger conduits are often associated with more flexible pit membranes of lower resistance to air-seeding-induced embolism (Pittermann et al. 2006, Domec et al. 2008, Hacke and Jansen 2009). Therefore, the relationship depicted in Figure 3A may be the consequence of larger conduits having bigger bordered pits, thus increasing the risk of cavitation.

Not surprisingly, the two broadleaved deciduous species tending to inhabit moist sites (*L. styraciflua* and *U. alata*) had the lowest resistance to embolism. The third species, *C. florida*, usually exhibits relatively little drought tolerance (Bahari et al. 1985, Hoffmann et al., personal communication). Nevertheless, our results showed that, compared with the other species, stems and roots of *C. florida* can withstand se-

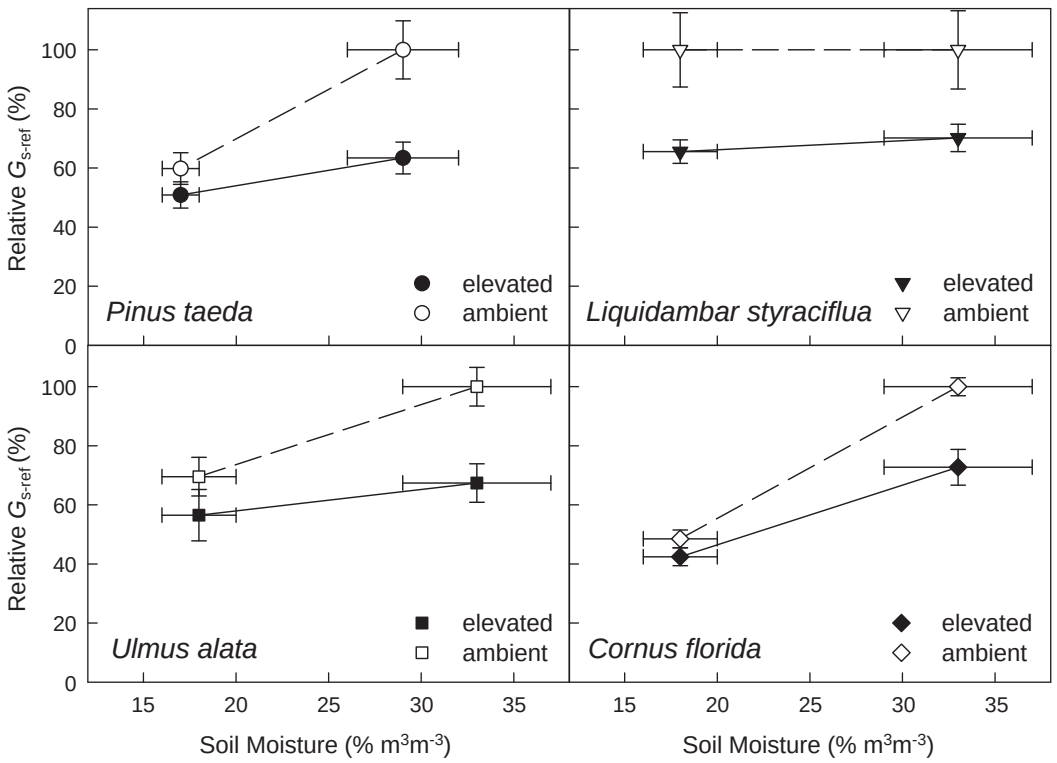

Figure 8. Effect of soil moisture on reference canopy stomatal conductance relative to the reference canopy stomatal conductance measured under ambient conditions and under high soil moisture (relative $G_{s\text{-ref}}$) in trees growing under either CO_2^a (ambient) or CO_2^e (elevated).

Downloaded from http://treephys.oxfordjournals.org at DigiTop USDA's Digital Desktop Library on August 24, 2010

vere drought before its xylem becomes severely impaired (Figure 5). There has been no study on leaf hydraulic vulnerability to embolism in this species, but we infer that in *C. florida* the weakest section of the hydraulic pathway is located in the petiole xylem, as evidenced from the rapid wilting, curling and leaf loss observed even during moderate droughts. In this species, leaves may act as a hydraulic fuse to protect the overall hydraulic system of the plant. We can refute the hypothesis of weak stomatal control to explain leaf wilting because this species had the strongest response of $G_{s\text{-ref}}$ to soil drying (Figure 8).

Over drying cycles or seasons in areas where soil moisture becomes progressively limited, the coordinated sensitivity between the liquid- and gas-phase fluxes coupled with treatment-induced differences in K_{tree} and $G_{s\text{-ref}}$ have consequences for gas exchange. It has been suggested that the responses of stomata to CO_2^e may vary with other environmental variables (Watanabe et al. 2008). Treatment-induced decreases in $G_{s\text{-ref}}$ was proportional to K_{tree} at a seasonal scale (Figure 7). *L. styraciflua* and, to a lesser degree, *U. alata* showed stomatal closure under CO_2^e regardless of soil moisture, consistent with previous studies (Gunderson et al. 2002, Herrick et al. 2004). In *L. styraciflua*, a reduction in stomatal density under CO_2^e was found at our site (Reid et al. 2003), perhaps explaining the reduction observed in $G_{s\text{-ref}}$. However, in *C. florida*, CO_2-induced decrease in $G_{s\text{-ref}}$ was greater in moist than in dry soil (Table 3), possibly reflecting a greater fine root density at the lower end of the rooting zone under CO_2^e (King et al. 2001, Pritchard et al. 2008). In *P. taeda*, there was no response of $G_{s\text{-ref}}$ to CO_2^e in 2000, 3 years after fumigation began, but $G_{s\text{-ref}}$ was appreciably reduced in 2007 (Table 3). Studies detected stomatal closure in most broadleaved species (Murthy et al. 1996, Saxe et al. 1998) but a more variable response in conifers, with a tendency for the longer studies to demonstrate an effect (Medlyn et al. 2001, Domec et al. 2009*c*). In conifers with many sapwood rings, the length of exposure to CO_2^e necessary to produce a reduction in K_{tree} and thus $G_{s\text{-ref}}$ may depend on the time it takes the species to replace a large proportion of pre-treatment hydro-active xylem with that produced under CO_2^e. This lag effect of fumigation on whole wood structure and thus physiology could explain the response of *P. taeda* in 2000 versus 2007 under high soil moisture (Table 3). In 2000, few of the total functional rings may have been produced under CO_2^e, so K_{tree} represented an integrated mean of K_{tree} under CO_2^a and under CO_2^e, whereas in 2007 it is expected that most rings of active xylem were produced under CO_2^e, allowing a significant difference in K_{tree} and $G_{s\text{-ref}}$ to be detected. Hydraulic determinants of wood structure are more complex in angiosperms than in conifers (McCulloh et al. 2010). In ring-porous species and to some extent in diffuse-porous species, the youngest rings are the most efficient at moving water and represent most of the hydraulically active sapwood (Phillips et al. 1996). Thus, we do not expect any lag effect of fumigation in the angiosperms, and the responses to CO_2^e we reported for 2000 were not predicted to change as trees got older.

The hydraulic adjustments resulted in changes in the sensitivity of $G_{s\text{-ref}}$ and, by extension, gas exchange to decreasing soil moisture (Figure 8). However, whereas *P. taeda*, *C. florida* and to some extent *U. alata* hydraulically adjusted under CO_2^e such that their gas exchange could be better maintained as soil moisture decreased compared with CO_2^a, adjustments of *L. styraciflua* were insufficient or cancelling, such that their stomata remained as sensitive to drying soil as under CO_2^a (Figure 8). This implies that, in addition to other advantages *P. taeda* will gain under CO_2^e (LaDeau and Clark 2001), hydraulic adjustments will allow it to keep photosynthesizing well under dry soil conditions.

Structure–function relationships in branches versus roots

From roots to branches, trade-offs existed such that the more distal parts were more resistant to air-seeding but at the cost of lower mean hydraulic diameter and consequently lower $k_{s\text{-max}}$ (Ewers et al. 2000). These changes in the hydraulic architecture along the pathway from roots to branches is consistent with decreasing water potential from the base to the apex of trees (Tyree and Ewers 1991, Domec and Gartner 2002, Choat et al. 2005).

Because P_{50} pooled over roots and branches of all species was correlated with wood density, the latter can be used as an index of drought resistance (Hacke et al. 2001*a*, Hacke and Jansen 2009). However, as previously discussed (Rosner et al. 2007, Domec et al. 2009*b*), wood density is an integrated average of earlywood and latewood densities weighted by their respective proportion within an annual ring, whereas the hydraulic characteristics of the whole sample (earlywood and latewood combined) are mostly a reflection of earlywood hydraulic properties. Low resistance to embolism may simply reflect the fact that rings with lower wood density contain earlywood made of wider conduits and thinner cell walls relative to their lumen (Panshin and deZeeuw 1980). Therefore, high wood density may not necessarily be correlated with high resistance to embolism.

Contrary to roots, branches have to resist the mechanical stresses induced by gravity, wind and ice loading, which tend to produce denser wood (James et al. 2006, Read and Stokes 2006). At the cell level, this translates to overbuilt conduits of thicker cell wall and higher $(t/b)^2$ (Sperry et al. 2006, Domec et al. 2009*b*, Hacke and Jansen 2009) that is often associated with lower conductivity but also with less flexible pit membranes of greater resistance to air-seeding-induced embolism (Domec et al. 2008, Hacke and Jansen 2009). Therefore, our branches had smaller $k_{s\text{-pit}}$ probably caused by smaller bordered pits and the associated less conductive pores in the cell membrane, together constraining the conductivity of the pit. Structurally, these pits have a greater potential to seal more effectively, thereby reducing the risk of cavitation (Hacke et al. 2004, Domec et al. 2006, Pittermann et al. 2006). The differences in biomechanical demands imposed on roots and branches may also explain why two distinct relationships relating P_{50} to $k_{s\text{-max}}$ emerged (Figure 2B). It should also be

Downloaded from http://treephys.oxfordjournals.org at DigiTop USDA's Digital Desktop Library on August 24, 2010

noted that end-wall resistivity was higher in *P. taeda* branches, highlighting the key differences between angiosperm and conifer pit membranes (Pittermann et al. 2005, Choat et al. 2008). Because values of $k_{s\text{-max}}$ in branches were more pit dependent than in roots, anatomical features enhancing cavitation resistance would require changes in pit structure that reduce pit conductivity and thus $k_{s\text{-max}}$. In turn, pit structural features responsible for lowering P_{50} will also cause higher flow resistance and therefore steeper pressure gradients and more negative xylem pressures, assuming no other adjustments (such as stomatal closure or higher root or sapwood area per leaf area). These features that lowered P_{50} would then require even stronger cell walls to avoid collapse, consistent with branches having higher $(t/b)^2$ making cell walls less likely to implode. Based on the range of $(t/b)^2$ determined in this study and the formulae in Hacke et al. (2001*a*, 2004), we estimated that actual implosion pressure would be in the range of 2.0–3.6 MPa in roots and 2.5–10 MPa in branches. One interpretation of such high implosion pressures compared with actual xylem pressures is that there has been strong selection pressure to avoid implosion (Pittermann et al. 2006, Hacke and Jansen 2009) probably because, contrary to air seeding, cell wall implosion would cause irreversible hydraulic failure. The observed increase in $(t/b)^2$ of the two canopy species (Table 3) is consistent with the lower P_{50} observed in roots of these species (Figure. 1) but, given the analysis above, may not represent a meaningful increase in protection against implosion.

Conclusions

Changes in CO_2 concentration of the earth's atmosphere (Keeling et al. 1995) and precipitation regimes (Gregory et al. 1997) are affecting current tree growth and wood quality (Ceuleman et al. 2002). Utilizing unique experimental settings such as FACE to examine the effect of water stress on trees under CO_2^e increases our ability to forecast future environmental impacts on tree and forest function and productivity (Schäfer et al. 2003, McCarthy et al. 2007, 2009). We show that in some species CO_2^e altered the hydraulic pathway, most likely structurally, affecting the liquid phase transport and consequently reducing stomatal conductance. This contrasts with previous studies focusing on a direct stomatal response to CO_2^e. We also show evidence that the hydraulic changes allow plants growing under CO_2^e to be less affected by drought than plants growing under current CO_2. These findings suggest that hydraulic adjustments to CO_2^e or their consequences to gas exchange and species competitive stance must be incorporated in models employed to predict forest responses to climate change.

Acknowledgments

We thank Uwe Hacke for helping with the anatomy data and for providing helpful comments on an earlier draft. John Sperry is gratefully acknowledged for letting us use his centrifuge to run the vulnerability curves.

Funding

This research was sponsored by the Office of Science (BER), US Department of Energy (FG02-95SER62083).

References

Addington, R.N., R.J. Mitchell, R. Oren and L.A. Donovan. 2004. Stomatal sensitivity to vapor pressure deficit and its relationship to hydraulic conductance in *Pinus palustris*. Tree Physiol. 24: 561–569.

Ainsworth, E.A. and A. Rogers. 2007. The response of photosynthesis and stomatal conductance to rising [CO_2]: mechanisms and environmental interactions. Plant Cell Environ. 30: 258–270.

Alder, N.N., W.T. Pockman, J.S. Sperry and S. Nuismer. 1997. Use of centrifugal force in the study of xylem cavitation. J. Exp. Bot. 48:665–674.

Atkinson, C.J. and J.M. Taylor. 1996. Effects of elevated CO_2 on stem growth, vessel area and hydraulic conductivity of oak and cherry seedlings. New Phytol. 133:617–626.

Bahari, Z.A., S.G. Pallardy and W.C. Parker. 1985. Photosynthesis, water relations, and drought adaptation in six woody species of oak-hickory forests in central Missouri. For. Sci. 31:557–569.

Ceulemans, R., M.E. Jach, R. van de Velde, J.X. Lin and M. Stevens. 2002. Elevated atmospheric CO_2 alters wood production, wood quality and wood strength of Scots pine (*Pinus sylvestris* L.) three years of enrichment. Global Change Biol. 8:153–162.

Cochard, H., L. Coll, X. Le Roux and T. Améglio. 2002. Unraveling the effects of plant hydraulics on stomatal closure during water stress in walnut. Plant Physiol. 128:282–290.

Choat, B., E.C. Lahr, P.J. Melcher, M.A. Zwieniecki and N.M. Holbrook. 2005. The spatial pattern of air seeding thresholds in mature sugar maple trees. Plant Cell Environ. 28:1094–1102.

Choat, B., A.R. Cobb and S. Jansen. 2008. Structure and function of bordered pits: new discoveries and impacts on whole-plant hydraulic function. New Phytol. 177:608–626.

Comstock, J.P. 2002. Hydraulic and chemical signalling in the control of stomatal conductance and transpiration. J. Exp. Bot. 53:195–200.

Conroy, J.P., M. Küppers, B. Küppers, J. Virgona and E.W.R. Barlow. 1988. The influence of CO_2 enrichment, phosphorus deficiency and water stress on the growth, conductance and water use of *Pinus radiata* D Don.. Plant Cell Environ. 11:91–98.

Domec, J.-C. and B.L. Gartner. 2001. Cavitation and water storage capacity in bole xylem segments of mature and young Douglas-fir trees. Trees 15:204–214.

Domec, J.-C. and B.L. Gartner. 2002. Age- and position-related changes in hydraulic versus mechanical dysfunction of xylem: inferring the design criteria for Douglas-fir wood structure. Tree Physiol. 22:91–104.

Domec, J.-C., J.M. Warren, F.C. Meinzer, J.R. Brooks and R. Coulombe. 2004. Native root xylem embolism and stomatal closure in stands of Douglas-fir and ponderosa pine: mitigation by hydraulic redistribution. Oecologia 141:7–16.

Domec, J.-C., F.G. Scholz, S.J. Bucci, F.C. Meinzer, G. Goldstein and R. Villalobos-Vega. 2006*a*. Diurnal and seasonal variation in root xylem embolism in neotropical savanna woody species: impact on stomatal control of plant water status. Plant Cell Environ. 29:26–35.

Domec, J.-C., B. Lachenbruch and F.C. Meinzer. 2006*b*. Bordered pit structure and function determine spatial patterns of air-seeding

Downloaded from http://treephys.oxfordjournals.org at DigiTop USDA's Digital Desktop Library on August 24, 2010

thresholds in xylem of Douglas-fir (*Pseudotsuga menziesii*; Pinaceae) trees. Am. J. Bot. 93:1600–1610.

Domec, J.-C., B. Lachenbruch, F.C. Meinzer, D.R. Woodruff, J.M. Warren and K.A. McCulloh. 2008. Maximum height in a conifer is associated with conflicting requirements for xylem design. Proc. Natl. Acad. Sci. USA 105:12069–12074.

Domec, J.-C., A. Noormets, J.S. King, G. Sun, S.G. McNulty, M. Gavazzi, J. Boggs and E. Treasure. 2009*a*. Decoupling the influence of leaf and root hydraulic conductances on stomatal conductance and its sensitivity to vapor pressure deficit as soil dries in a drained loblolly pine plantation. Plant Cell Environ. 32:980–991.

Domec, J.-C., J. Warren, B. Lachenbruch and F.C. Meinzer. 2009*b*. Safety factors from air seeding and cell wall implosion in young and old conifer trees. IAWA J. 30:100–120.

Domec, J.-C., S. Palmroth, E. Ward, C.A. Maier, M. Thérézien and R. Oren. 2009*c*. Acclimation of leaf hydraulic conductance and stomatal conductance of *Pinus taeda* (loblolly pine) to long term growth in elevated CO_2 (FACE) and N-fertilization. Plant Cell Environ. 32:1500–1512.

Ellsworth, D.S., R. Oren, C. Huang, N. Phillips and G.R. Hendrey. 1995. Leaf and canopy responses to elevated CO_2 in a pine forest under free-air CO_2 enrichment. Oecologia 104:139–146.

Ewers, F.W. 1985. Xylem structure and water conduction in conifer trees, dicot trees and lianas. IAWA Bull. 6:309–317.

Ewers, B.E. and R. Oren. 2000*a*. Analyses of assumptions and errors in the calculation of stomatal conductance from sap flux measurements. Tree Physiol. 20:579–589.

Ewers, B., R. Oren and J.S. Sperry. 2000*b*. Influence of nutrient versus water supply on hydraulic architecture and water balance in *Pinus taeda*. Plant Cell Environ. 23:1055–1066.

Gartner, B.L., J. Roy and R. Huc. 2003. Effects of tension wood on specific conductivity and vulnerability to embolism of *Quercus ilex* seedlings grown at two atmospheric CO_2 concentrations. Tree Physiol. 23:387–395.

Granier, A. 1987. Evaluation of transpiration in a Douglas-fir stand by means of sap flow measurements. Tree Physiol. 3:309–320.

Gregory, J.M., J.F.B. Mitchell and A.J. Brady. 1997. Summer drought in northern midlatitudes in a time-dependent CO_2 climate experiment. J. Climate 10:662–686.

Gunderson, C.A., J.D. Sholtis, S.D. Wullschleger, D.T. Tissue, P.J. Hanson and R.J. Norby. 2002. Environmental and stomatal control of photosynthetic enhancement in the canopy of a sweetgum (*Liquidambar styraciflua* L.) plantation during three years of CO_2 enrichment. Plant Cell Environ. 25:379–393.

Hacke, U.G. and S. Jansen. 2009. Embolism resistance of three boreal conifer species varies with pit structure. New Phytol. 182:675–686.

Hacke, U.G., J.S. Sperry, B.E. Ewers, D.S. Ellsworth, K.V.R. Schäfer and R. Oren. 2000. Influence of soil porosity on water use in *Pinus taeda*. Oecologia 124:495–505.

Hacke, U.G., J.S. Sperry, W.T. Pockman, S.D. Davis and K.A. McCulloh. 2001*a*. Trends in wood density and structure are linked to prevention of xylem implosion by negative pressure. Oecologia 126:457–461.

Hacke, U.G., V. Stiller, J.S. Sperry, J. Pittermann and K.A. McCulloh. 2001*b*. Cavitation fatigue: embolism and refilling cycles can weaken cavitation resistance of xylem. Plant Physiol. 125:779–786.

Hacke, U.G., J.S. Sperry and J. Pittermann. 2004. Analysis of circular bordered pit function II. Gymnosperm tracheids with torus-margo pit membranes. Am. J. Bot. 91:386–400.

Hacke, U.G., J.S. Sperry, J.K. Wheeler and L. Castro. 2006. Scaling of angiosperm xylem structure with safety and efficiency. Tree Physiol. 26:689–701.

Hendrey, G.R., D.S. Ellsworth, K.F. Lewin and J. Nagy. 1999. A free-air enrichment system for exposing tall forest vegetation to elevated atmospheric CO_2. Global Change Biol. 5:293–310.

Herrick, J.D., H. Maherali and R.B. Thomas. 2004. Reduced stomatal conductance in sweetgum (*Liquidambar styraciflua*) sustained over long-term CO_2 enrichment. New Phytol. 162:243–561.

James, K.R., N. Haritos and P.K. Ades. 2006. Mechanical stability of trees under dynamic loads. Am. J. Bot. 2006:1522–1530.

Jones, H.G. 1992. Plants and microclimate: a quantitative approach to environmental plant physiology. Cambridge University Press, Cambridge, UK.

Kaakinen, S., K. Kostiainen, F. Ek, P. Saranpää, M.E. Kubiske, J. Sober, D.F. Karnosky and E. Vapaavuori. 2004. Stem wood properties of *Populus tremuloides*, *Betula papyrifera* and *Acer saccharum* saplings after 3 years of treatments to elevated carbon dioxide and ozone. Global Change Biol. 10:1513–1525.

Kim, H.-S. 2009. Measurement and modeling of radiation and water fluxes in plantation forests. PhD dissertation. Duke University, Durham, NC.

Kim, H.-S., R. Oren and T.M. Hinckley. 2008. Actual and potential transpiration and carbon assimilation in an irrigated poplar plantation. Tree Physiol. 28:559–577.

King, J.S., K.S. Pregitzer, D.R. Zak, J. Sober, J.G. Isebrands, R.E. Dickson, G.R. Hendrey and D.F. Karnosky. 2001. Fine-root biomass and fluxes of soil carbon in young stands of paper birch and trembling aspen as affected by elevated atmospheric CO_2 and tropospheric O_3. Oecologia 128:237–250.

Keeling, C.D., T.P. Whorf, M. Wahlen and J. van der Plicht. 1995. Interannual extremes in the rate of rise of atmospheric carbon dioxide since 1980. Nature 375:666–670.

Kolb, K.J. and J.S. Sperry. 1999. Differences in drought adaptation between subspecies of sagebrush (*Artemisia tridentata*). Ecology 80:2373–2384.

Köstner, B.M.M., E.-D. Schulze, F.M. Kelliher, D.Y. Hollinger, J.N. Byers, J.E. Hunt, T.M. McSeveny, R. Meserth and P.L. Weir. 1992. Transpiration and canopy conductance in a pristine broad-leaved forest of *Nothofagus*: an analysis of xylem sap flow and eddy correlation measurements. Oecologia 91:350–359.

Kupper, P., A. Sellin, Z. Klimánková, R. Pokorný and J. Puértolas. 2006. Water relations in Norway spruce trees growing at ambient and elevated CO_2 concentrations. Biol. Plant. 50:594–603.

LaDeau, S. and J. Clark. 2001. Rising CO_2 levels and the fecundity of forest trees. Science 292:95–98.

Loustau, D., J.-C. Domec and A. Bosc. 1998. Interpreting the variations in xylem sap flux density within the trunk of maritime pine (*Pinus pinaster* Ait.): application of a model for calculating water flows at tree and stand levels. Ann. Sci. For. 55:29–46.

Maseda, P.H. and R.J. Fernández. 2006. Stay wet or else: three ways in which plants can adjust hydraulically to their environment. J. Exp. Bot. 57:3963–3977.

McCarthy, H.R., R. Oren, H.S. Kim, K.H. Johnsen, C. Maier, S.G. Pritchard and M.A. Davis. 2006. Interaction of ice storms and management practices on current carbon sequestration in forests with potential mitigation under future CO_2 atmosphere. J. Geophys. Res. 111:101029/2005JD006428.

McCarthy, H.R., R. Oren, A.C. Finzi, D.S. Ellsworth, H.S. Kim, K.H. Johnson and B. Millar. 2007. Temporal dynamics and spatial variability in the enhancement of canopy leaf area

Downloaded from http://treephys.oxfordjournals.org at DigiTop USDA's Digital Desktop Library on August 24, 2010

under elevated atmospheric CO_2. Global Change Biol. 13:2479–2497.

McCarthy, H.R., R. Oren, K.H. Johnsen, A. Gallet-Budynek, S.G. Pritchard, C.W. Cook, S.L. LaDeau, R.B. Jackson and A.C. Finzi. 2009. Re-assessment of plant carbon dynamics at the Duke free-air CO_2 enrichment site: interactions of atmospheric [CO_2] with nitrogen and water availability over stand development. New Phytol. DOI: 10.1111/j.1469-8137.2009.03078.

McCully, M.E., C.X. Huang and L.E. Ling. 1998. Daily embolism and refilling of xylem vessels in the roots of field-grown maize. New Phytol. 138:327–342.

McCulloh, K., J.S. Sperry, B. Lachenbruch, F.C. Meinzer, P.B. Reich and S. Voelker. 2010. Moving water well: comparing hydraulic efficiency in twigs and trunks of coniferous, ring-porous, and diffuse-porous saplings from temperate and tropical forest. New Phytol. 186:439–450.

Medlyn, B.E., B.E. Medlyn, B.E. Medlyn et al. 2001. Stomatal conductance of forest species after long-term exposure to elevated CO_2 concentration: a synthesis. New Phytol. 149:247–264.

Meinzer, F.C. 2002. Co-ordination of vapour and liquid phase water transport properties in plants. Plant Cell Environ. 25:265–274.

Meinzer, F.C., D.M. Johnson, B. Lachenbruch, K.A. McCulloh and D.R. Woodruff. 2009. Xylem hydraulic safety margins in woody plants: coordination of stomatal control of xylem tension with hydraulic capacitance. Funct. Ecol. 23:922–930.

Monje, O. and B. Bugbee. 1998. Adaptation to high CO_2 concentration in an optimal environment: radiation capture, canopy quantum yield and carbon use efficiency. Plant Cell Environ. 21:315–324.

Monteith, J.L. and M.H. Unsworth. 1990. Principles of environmental physics. Edward Arnold, London, 291 p.

Murthy, R., P.M. Dougherty, S.J. Zarnoch and H.L. Allen. 1996. Effects of carbon dioxide, fertilization, and irrigation on photosynthetic capacity of loblolly pine trees. Tree Physiol. 16:537–546.

Norby, R.J. and R.B. Jackson. 2000. Root dynamics and global change: seeking an ecosystem perspective. New Phytol. 147: 3–12.

Novick, K., R. Oren, P. Stoy, P.M. Siqueira and G.G. Katul. 2009. Nocturnal evapotranspiration in eddy-covariance records from three co-located ecosystems in the Southeastern U.S.: Implications for annual fluxes. Agric. For. Meteorol. 149: 1491–1504.

Oishi, A.C., R. Oren and P.C. Stoy. 2008. Estimating components of forest evapotranspiration: a footprint approach for scaling sap flux measurements. Agric. For. Met. 148:719–732.

Oren, R., B.E. Ewers, P. Todd, N. Phillips and G. Katul. 1998*a*. Water balance delineates the soil layer in which soil moisture affects canopy conductance. Ecol. Appl. 8:990–1002.

Oren, R., N. Phillips, G. Katul, B.E. Ewers and D.E. Pataki. 1998*b*. Scaling xylem sap flux and soil water balance and calculating variance: a method for partitioning water flux in forests. Ann. Sci. For. 55:191–216.

Oren, R., J.S. Sperry, G.G. Katul, D.E. Pataki, B.E. Ewers, N. Phillips and K.V.R. Schäfer. 1999. Survey and synthesis of intra- and interspecific variation in stomatal sensitivity to vapour pressure deficit. Plant Cell Environ. 22:1515–1526.

Oren, R., D.S. Ellsworth, K.H. Johnsen et al. 2001. Soil fertility limits carbon sequestration by forest ecosystems in a CO_2-enriched atmosphere. Nature 411:469–472.

Pammenter, N.W. and C. Vander Willigen. 1998. A mathematical and statistical analysis of the curves illustrating vulnerability of xylem to cavitation. Tree Physiol. 18:589–593.

Panshin, A.J. and C. de Zeeuw. 1980. Textbook of wood technology 4th Edn. McGraw-Hill, New York, 722 p.

Pataki, D.E. and R. Oren. 2003. Species differences in stomatal control of water loss at the canopy scale in a mature bottomland deciduous forest. Adv. Water Res. 26:1267–1278.

Pataki, D.E., R. Oren and N. Phillips. 1998*a*. Responses of sap fux and stomatal conductance of *Pinus taeda* L. trees to stepwise reductions in leaf area. J. Exp. Bot. 49:871–878.

Pataki, D.E., R. Oren and P. Tissue. 1998*b*. Elevated carbon dioxide does not affect average canopy stomatal conductance of *Pinus taeda* L. Oecologia 117:47–52.

Phillips, N., R. Oren and R. Zimmermann. 1996. Radial pat terns of xylem sap flow in non diffuse- and ring- porous tree species. Plant Cell Environ. 19:983–990.

Phillips, N., A. Nagchaudhuri, R. Oren and G. Katul. 1997. Time constant for water transport in loblolly pine trees estimated from time series of evaporative demand and stem sapflow. Trees 11:419.

Pittermann, J., J.S. Sperry, U.G. Hacke, J.K. Wheeler and E. Sikkema. 2005. Torus-margo pits help conifers compete with angiosperms. Science 310:1924.

Pittermann, J., J.S. Sperry, J.K. Wheeler, U.G. Hacke and E. Sikkema. 2006. Mechanical reinforcement against tracheid implosion compromises the hydraulic efficiency of conifer xylem. Plant Cell Environ. 29:1618–1628.

Pritchard, S.G., A.E. Strand, M.L. McCormack, M.A. Davis, A.C. Finzi, R.B. Jackson, R. Matamala, H.H. Rogers and R. Oren. 2008. Fine root dynamics in a loblolly pine forest are influenced by free-air-CO_2-enrichment: a six-year-minirhizotron study. Global Change Biol. 14:588–602.

Read, J. and A. Stokes. 2006. Plant biomechanics in an ecological context. Am. J. Bot. 93:1546–1565.

Reid, C.D., H. Maherali, H.B. Johnson, S.D. Smith, S.D. Wullschleger. and R.B. Jackson. 2003. On the relationship between stomatal characters and atmospheric CO_2. Geophys. Res. Lett. 30:1983, doi 10.1029/2003GL017775.

Rosner, S., A. Klein, U. Muller and B. Karlsson. 2007. Hydraulic and mechanical properties of young Norway spruce clones related to growth and wood structure. Tree Physiol. 27:1165–1178.

Saxe, H., D.S. Ellsworth and J. Heath. 1998. Tree and forest functioning in an enriched CO_2 atmosphere. New Phytol. 139:395–436.

Schäfer, K. 2009. Water and carbon relations under ambient and elevated atmospheric CO_2: water and carbon relations of temperate forest species under ambient and elevated atmospheric CO_2 conditions VDM Verlag, Dr. Muller Aktiengesellschaft & Co., 144 p.

Schäfer, K.V.R., R. Oren, C.-T. Lai and G.G. Katul. 2002. Hydrologic balance in an intact temperate forest ecosystem under ambient and elevated atmospheric CO_2 concentration. Global Change Biol. 8:895–911.

Schäfer, K.V.R., R. Oren, D.S. Ellsworth, C.-T. Lai, J.D. Herrick, A.C. Finzi, D.D. Richter and G.G. Katul GG. 2003. Exposure to an enriched CO_2 atmosphere alters carbon assimilation and allocation in a pine forest ecosystem. Global Change Biol. 9: 1378–1400.

Sperry, J.S. 2000. Hydraulic constraints on plant gas exchange. Agric. For. Met. 104:13–23.

Sperry, J.S. and T. Ikeba. 1997. Xylem cavitation in roots and stems of Douglas-fir and white fir. Tree Physiol. 17:275–280.

Sperry, J.S., F.R. Adler, G.S. Campbell and J.P. Comstock. 1998. Limitation of plant water use by rhizosphere and xylem conductance: results from a model. Plant Cell Environ. 21:347–359.

Downloaded from http://treephys.oxfordjournals.org at DigiTop USDA's Digital Desktop Library on August 24, 2010

Sperry, J.S., U.G. Hacke and J. Pittermann. 2006. Size and function in conifer tracheids and angiosperm vessels. Am. J. Bot. 93: 1490–1500.

Sterck, F.K., R. Zweifel, U. Sass-Klaassen and Q. Chowdhury. 2008. Persisting soil drought reduces leaf specific conductivity in Scots pine (*Pinus sylvestris*) and pubescent oak (*Quercus pubescens*). Tree Physiol. 28:529–536.

Telewski, F.W., T. Swanson, E.R. Strain and J.M. Burns. 1999. Wood properties and ring width responses to long-term atmospheric CO_2 enrichment in field-grown loblolly pine (*Pinus taeda*). Plant Cell Environ. 22:213–219.

Tyree, M.T. and J.D. Alexander. 1993. Plant water relations and the effects of elevated CO_2: a review and suggestions for future research. Vegetatio 104:47–62.

Tyree, M.T. and F.W. Ewers. 1991. The hydraulic architecture of trees and other woody plants. New Phytol. 119:345–360.

Tyree, M.T. and M.H. Zimmermann. 2002. Xylem structure and the ascent of sap. 2nd edn., Springer, New York, 345 p.

Ward, E.J., R. Oren, B.D. Sigurdsson, P.G. Jarvis and S. Linder. 2008. Fertilization effects on mean stomatal conductance are mediated through changes in the hydraulic attributes of mature Norway spruce trees. Tree Physiol. 28:579–596.

Watanabe, Y., H. Tobita, M. Kitao and Y. Maruyama. 2008. Effects of elevated CO_2 and nitrogen on wood structure related to water transport in seedlings of two deciduous broad-leaved tree species. Trees 22:403–411.

Woodward, F.I. 1993. Plant responses to past concentrations of CO_2. Plant Ecol. 104:145–155.

Downloaded from http://treephys.oxfordjournals.org at DigiTop USDA's Digital Desktop Library on August 24, 2010